Expansion of human hematopoietic stem cells by inhibiting translation

Chenchen Li[1]*, Hanna Shin[1]*, Dheeraj Bhavanasi[1], Mai Liu[2], Xiang Yu[3], Scott A. Peslak[1,4], Xiaolei Liu[1], Juan R. Alvarez-Dominguez[2,5], Gerd A. Blobel[4], Brian D. Gregory[3], Jian Huang[6,7], Peter S. Klein[1,2,5‡]

[1]Division of Hematology-Oncology, Department of Medicine, Perelman School of Medicine, University of Pennsylvania, Philadelphia, PA 19104, USA.

[2]Department of Cell and Developmental Biology, Perelman School of Medicine, University of Pennsylvania, Philadelphia, PA 19104, USA.

[3]Department of Biology, University of Pennsylvania, Philadelphia, PA 19104, USA

[4]Division of Hematology, The Children's Hospital of Philadelphia, Philadelphia, PA 19104, USA.

[5]Institute for Regenerative Medicine, Perelman School of Medicine, University of Pennsylvania, Philadelphia, PA 19104, USA.

[6]Coriell Institute for Medical Research; Camden, NJ, 08103, USA.

[7]Cooper Medical School of Rowan University, Camden, NJ, 08103, USA.

‡Corresponding author: pklein@pennmedicine.upenn.edu

*These authors contributed equally.

Keywords: hematopoietic stem cell, hematopoietic stem cell transplantation, umbilical cord blood, glycogen synthase kinase-3, mTORC1, Translation, eIF4E, gene editing, gene therapy, sickle cell disease, unfolded protein response,

Abstract

Hematopoietic stem cell (HSC) transplantation using umbilical cord blood (UCB) is a potentially life-saving treatment for leukemia and bone marrow failure but is limited by the low number of HSCs in UCB. The loss of HSCs after ex vivo manipulation is also a major obstacle to gene editing for inherited blood disorders. HSCs require a low rate of translation to maintain their capacity for self-renewal, but hematopoietic cytokines used to expand HSCs stimulate protein synthesis and impair long-term self-renewal. We previously described cytokine-free conditions that maintain but do not expand human and mouse HSCs ex vivo. Here we performed a high throughput screen and identified translation inhibitors that allow ex vivo expansion of human HSCs while minimizing cytokine exposure. Transplantation assays show a ~5-fold expansion of long-term HSCs from UCB after one week of culture in low cytokine conditions. Single cell transcriptomic analysis demonstrates maintenance of HSCs expressing mediators of the unfolded protein stress response, further supporting the importance of regulated proteostasis in HSC maintenance and expansion. This expansion method maintains and expands human HSCs after CRISPR/Cas9 editing of the *BCL11A+58* enhancer, overcoming a major obstacle to ex vivo gene correction for human hemoglobinopathies.

Hematopoietic stem cells (HSCs) are primarily quiescent but on demand are capable of expansion and differentiation into multiple lineages. Quiescent HSCs maintain a low rate of protein synthesis compared to more differentiated hematopoietic cells[1,2], whereas activation of HSCs is associated with increased translation and restriction of self-renewal capacity. HSCs have a limited capacity to survive outside of the complex hematopoietic niche and traditionally have been supported in culture by the addition of multiple hematopoietic cytokines, which promote survival but also drive proliferation, lineage commitment, and the loss of self-renewing, long-term HSCs (LT-HSCs)[3,4].

HSC transplantation (HSCT) can be a life-saving therapy for hematological neoplasms and bone marrow failure but is constrained by the limited availability of suitably matched donors, especially for ethnic groups that are underrepresented in bone marrow registries[5,6]. While haploidentical transplants help to address this issue[7,8], umbilical cord blood (UCB) remains a valuable and underutilized[9] resource for human HSCs that requires reduced stringency in HLA matching and has a reduced risk of graft vs host disease[9-16]. UCB units, however, typically contain a low number of HSCs, resulting in delayed neutrophil and platelet engraftment. The use of two UCB donors can improve the rate of neutrophil engraftment, but is associated with immunological extinction of one of the two donors, increased graft versus host disease, impaired platelet recovery[17], and substantially increased cost. Thus, even modest expansion of HSCs in existing UCB units would dramatically increase the number of UCB units available for genetically diverse patients needing HSCT.

Approaches to expand HSCs in UCB have relied on cocktails of hematopoietic cytokines combined with an array of factors, including UM171, nicotinamide, the aryl hydrocarbon receptor antagonist SR1, the PPAR-γ antagonist GW9662, zwitterionic hydrogels, polyvinyl alcohol (PVA), histone deacetylase inhibitors, BET inhibitors, Notch ligands, angiopoietin-like proteins, pleiotrophin, and others[18-33]. A subset of these approaches was validated with limiting dilution transplant assays and serial transplantation in immunocompromised mice. A formulation using $CD133^+$ cells isolated from UCB, cultured with nicotinamide and multiple cytokines, and then combined with the $CD133^-$ fraction (termed Omidubicel) showed improved neutrophil and platelet recovery compared to single or double unit UCB transplants in a phase 3 trial[32] and has been FDA approved for use in hematopoietic malignancies. SR1 and UM171 have also shown promising data in early phase clinical trials[34,35]. However, all of these HSC expansion conditions depend on high concentrations of multiple cytokines or small molecule activators of cytokine signaling, incurring the potential for activating protein synthesis and driving cells into lineage commitment[19,20,31,36-38].

To circumvent the loss of self-renewal associated with cytokine activation, we have explored cytokine-free conditions for the ex vivo maintenance of HSCs. Human or mouse LT-HSCs can be maintained ex vivo without cytokines, support cells, or serum when the signaling kinases glycogen synthase kinase 3 (GSK-3) and mechanistic target of rapamycin complex 1 (mTORC1) are inhibited[39-41]. In vivo limiting dilution assays showed no loss of long-term reconstituting activity in these cytokine-free conditions. However, the absolute number of LT-HSCs was not substantially increased. To identify an approach to expand LT-HSCs ex vivo, we performed a high throughput chemical screen based on our previously described HSC culture conditions[40] modified to include a mitogenic stimulus while minimizing cytokine exposure. The screen identified multiple inhibitors of translation initiation, consistent with published evidence that HSCs restrict translation to maintain long-term self-renewal[1,2,42-48]. However, pharmacological inhibition of translation has not previously been tested for therapeutic expansion of human HSCs. Here we show that pharmacological inhibition of translation paired with limited exposure to hematopoietic cytokines yields ex vivo expansion of human LT-HSCs.

Results

Maintenance of an HSC signature ex vivo

LT-HSCs can be maintained in cytokine-free medium for at least 7 days by inhibiting GSK-3 and mTORC1[39,40] but undergo limited cell division in the absence of mitogenic stimuli. To achieve a modest expansion of HSCs, we tested multiple combinations of common hematopoietic cytokines to find conditions that would minimize cytokine exposure and still allow expansion of $CD34^+$ cells in the presence of GSK-3 and mTORC1 inhibitors (CHIR99021 and Rapamycin (CR)). We found that limiting the cocktail to 3 cytokines (stem cell factor (SCF), thrombopoietin (TPO), and interleukin-3 (IL-3)) was sufficient to achieve expansion in the presence of CR (Supplemental Figure 1A). Most HSC expansion methods use cytokines such as SCF and TPO at ≥ 100 ng/ml[18-33]. We therefore tested different concentrations of SCF, TPO, and IL-3 (STI) to identify low cytokine concentrations that would still induce detectable proliferation in CR-containing medium (Supplemental Figure 1B). Robust expansion of $CD34^+$ cells was detected with SCF and TPO at 12.5 ng/ml and IL-3 at 1.25 ng/ml (Supplemental Figure 1C) in CR medium, and these low cytokine conditions (CRCY) were selected for further study.

To examine in more detail how subpopulations of hematopoietic cells are maintained upon culture in CR, we performed single-cell RNA sequencing (scRNA-seq). As $CD34^+$ cells from human UCB are heterogeneous, and only a small fraction are functional LT-HSCs, we enriched for HSCs using fluorescence activated cell sorting (FACS) of $CD34^+CD38^-CD45RA^-CD90^+$ cells[49]. Sorted cells were then analyzed immediately (uncultured control/day 0) or cultured for two days in STEM-Span medium with vehicle control (DMSO), CR, or CRCY, followed by scRNA-seq. Analysis of single cell data using Seurat identified 10 groups of cells, with several groups showing substantial overlap in gene expression. These groups were then annotated manually and each group was assigned a label based on their distinct markers yielding five main groups: hematopoietic stem cells and multipotent progenitor cells (HSC/MPPs), common myeloid progenitors (CMP), lymphoid-primed multipotent progenitors (LMPP), megakaryocyte-erythrocyte progenitors (MEP), and Early Erythroid Commitment (EEC). Uniform manifold approximation and projection (UMAP) visualization showed that, when compared to STEM-span medium, CR or CRCY maintains the HSC/MPP population present in freshly isolated cells (Day 0, Figure 1A and 1B). These single cell findings are consistent with our current and prior functional measures showing maintenance of HSCs cultured with CR.

Although there was overlap between the HSC/MPP and CMP groups in $CD34^+CD38^-CD45RA^-CD90^+$ cells, the HSC/MPP group was distinguished by the significantly higher expression of the unfolded protein response chaperone *GRP78/HSPA5*, several classical immediate early response (IER) genes (*IER2* and *NFKBIA*), and multiple members of the *JUN* transcription factor family (Figure 1C, Supplemental Table 1), which are associated with IER genes and regulators of the stress response through Jun kinases (JNKs). Indeed, *HSPA5* (Figure 1D) and *JUN* family members were among the most highly enriched genes in the HSC/MPP population compared to other hematopoietic subpopulations. Similarly, Gene Ontology (GO) analysis of the entire list of genes associated with the HSC/MPP population in CR-containing medium showed significant enrichment of genes related to the regulation of cellular response to stress and the unfolded protein response pathways (Figure 1E, Supplemental Table 2). A primary output of the unfolded protein response is to suppress translation[50]. The high expression of *HSPA5* and stress response genes is therefore consistent with the critical role of limited translation and proteostasis in HSC function[1,2,42,43].

High throughout screen with low cytokines

We performed a high-throughput screen (HTS) of 2,240 FDA approved and/or bioactive compounds to identify drugs that would enhance expansion of HSCs from UCB in the presence of CR and a low level of cytokines (Figure 2A, Supplemental Figure 1D). We identified 74 compounds that increase the number of $CD34^+$ cells > 1.4-fold and > 4 standard deviation units above the mean of control cells in CRCY alone in 2 replicate screens (Figure 2B, Supplemental Table 3) and 60 of these compounds were detected in a third replicate at 10-fold lower drug concentrations. Two compounds that directly inhibit the cap-dependent translation initiation factor eIF4E (4E1RCat and 4EGI-1) drew our attention because of prior work showing that suppression of cap-dependent translation is essential to maintain long-term HSCs in mice[2,43-45] and our scRNA-seq findings showing enrichment of UPR markers in the HSC/MPP pool. To validate these translation inhibitors further, we cultured human $CD34^+$ cells from UCB in CRCY with 4E1RCat, 4EGI-1, or the translation inhibitor 4E2RCat for 7 days and then performed flow cytometry (FCM) to detect phenotypic HSCs (pHSCs) based on the surface markers $CD34^+CD38^-CD45RA^-CD90^+CD49f^+$. pHSCs cultured in CRCY with 4E1RCat, 4E2RCat, or 4EGI-1 expanded up to ~10-fold compared to the number of pHSCs at Day 0 (Figure 2C), demonstrating dose-dependent expansion in the presence of eIF4E inhibitors. pHSC expansion was also significantly higher in CRCY+4E1RCat compared to CRCY alone. Therefore, we focused on 4E1RCat for functional studies of HSC expansion.

As the $CD34^+$ population contains HSCs and hematopoietic progenitor cells (HSPCs), we performed colony formation assays to assess the capacity of expanded HSPCs to differentiate into multilineage hematopoietic cell types. The number of colony-forming units (CFUs) generated from $CD34^+$ cells cultured in CRCY±4E1RCat increased 2-3 fold compared to uncultured cells (Figure 2D). The number of multipotent progenitors that generate granulocyte, erythroid, macrophage, and megakaryocyte lineages (CFU–GEMM) was significantly increased in the CRCY+4E1RCat group (Figure 2E). Thus CRCY+4E1RCat increases pHSCs and progenitor cell populations ex vivo.

We observe pHSC expansion with 4E1RCat at 2 μM, which is below the reported IC_{50} for inhibition of translation[51]. To confirm that 4E1RCat inhibits global translation in $CD34^+$ cells under these conditions, we measured protein synthesis by incorporation of the fluorescent puromycin analog O-propargyl-puromycin (OP-Puro) [2,52]. 4E1RCat decreased global translation in $CD34^+CD38^-CD90^+$ populations in a dose-dependent manner, with maximal inhibition between 2 μM and 10 μM (Figure 2F and 2G).

Expansion of functional HSCs

As a rigorous test of LT-HSC expansion by culture in CRCY+4E1RCat, we performed limiting dilution repopulation assays (LDA). $CD34^+$ cells at day 0 and cells cultured in CRCY±4E1RCat for 7 days were injected at varying cell doses into busulfan-conditioned non-obese diabetic severe combined immunodeficient IL-2Rγ^{null} (NSG) mice [40,53]. Bone marrow aspirates were collected at 20 weeks after transplantation and human cell chimerism was assessed by flow cytometry. The number of positive chimeric mice, defined as > 0.1% donor-derived human cells in bone marrow, was significantly higher in the group receiving $CD34^+$ cells cultured with 4E1RCat compared to the uncultured group and the group cultured in CRCY without 4E1RCat (Figure 3A; Supplemental Figure 2). The number of severe combined immunodeficiency (SCID)-repopulating cells (SRCs), a measure of the number of functionally engrafting human HSCs in cells cultured in CRCY+4E1RCat (1 in 242) was 4.9 fold higher than uncultured $CD34^+$ cells (1 in 1,188) (Figure 3B). No significant difference was observed with CRCY+DMSO (1 in 1,074) compared to the uncultured group (Figure 3A, B), consistent with HSC maintenance reported previously for CR medium [40]. Multi-lineage reconstitution was detected at 20 weeks in the 4E1RCat-treated group, as a substantial percentage of bone marrow cells were donor-derived,

including T cells ($CD3^+$), B cells ($CD19^+$), myeloid cells ($CD33^+$), and hematopoietic progenitor cells ($CD34^+CD38^-$) (Figure 3C-F), indicating that 4E1RCat confers multi-lineage reconstitution compared to the uncultured group.

To demonstrate further the capacity for long-term self-renewal after ex vivo expansion in CRCY+4E1RCat, we performed serial transplantation into secondary recipients using bone marrow cells harvested from five donors per condition at 29 weeks post-transplant (Figure 3G Supplemental Figure 3). Human chimerism was detected in the peripheral blood (PB) of secondary recipients in the 4E1RCat-treated group but not the uncultured group at 16 weeks post-transplant (Figure 3H). Bone marrow from secondary recipients at 18 weeks achieved a higher percentage of human chimerism ($hCD45^+$), hematopoietic progenitor cells ($CD34^+CD38^-$), B cells ($CD19^+$), myeloid cells ($CD33^+$), megakaryocytic cells ($CD41^+$), and erythroid cells ($GlyA^+$) compared to day 0 (uncultured) donor cells in secondary recipients (Figure 3I-N, Supplemental Figure 4). Thus, culture of UCB $CD34^+$ cells in CRCY+4E1RCat promotes the expansion of HSCs capable of long-term regeneration.

Expansion of CRISPR modified adult $CD34^+$ cells by 4E1RCat.

A major obstacle to therapeutic gene editing for inherited hematopoietic disorders such as sickle cell disease (SCD) is the loss of functional HSCs after culture in cytokine-rich media. Our approach could overcome this obstacle by maintaining and potentially expanding LT-HSCs during ex vivo manipulation. Human fetal red blood cells express primarily γ-globin chains that are paired with two α-globin chains to form fetal hemoglobin ($\gamma_2\alpha_2$; HbF). After birth the γ-globin (*HBG*) genes are transcriptionally silenced by repressors such as *BCL11A* and the β-globin gene (*HBB*) is activated to produce adult hemoglobin ($\beta_2\alpha_2$; HbA)[54,55]. Elevated HbF levels due to genetic variation or through therapeutic HbF inducers attenuate the severity of SCD. Thus, induction of HbF by directed targeting of the *BCL11A* repressor has been a long-standing goal in the field and recently has shown promising outcomes in treatment of SCD patients[56,57]. However, a major limitation of this approach is the limited number of viable $CD34^+$ cells that can be mobilized from patients and the loss of functional HSCs after ex vivo manipulations that typically involve exposure to high levels of multiple cytokines. Our low cytokine conditions could address these limitations by improving the ex vivo maintenance of HSCs and potentially increasing their numbers prior to autologous transplantation.

To test whether CRCY+4E1RCat can maintain or expand CRISPR/Cas9-edited HSCs, we targeted the *BCL11A* +58 erythroid enhancer in mobilized human $CD34^+$ cells from adult donors. Mobilized $CD34^+$ cells were edited with sgRNA targeting the erythroid-specific *BCL11A+58* enhancer and then cultured in CRCY±4E1RCat for 7 days. The absolute number of pHSCs increased 10 to 15-fold in non-edited and *BCL11A+58*-edited pHSCs, compared to uncultured cells (Figure 4A). Colony formation assays demonstrated that the capacity for hematopoietic differentiation also increased 3 to 5-fold in edited $CD34^+$ cells cultured in CRCY±4E1RCat (Figure 4B, C). Furthermore, CRCY+4E1RCat significantly increased the number of burst-forming unit-erythroid (BFU-E), granulocyte and macrophage CFUs (CFU-G/M/GM), and multipotent progenitors (CFU–GEMM) compared to CRCY or uncultured cells. Importantly, upon in vitro erythroid differentiation, *BCL11A+58*-edited cells treated with CRCY+4E1RCat maintained robust HbF induction (Figure 4D) without disruption of erythroid maturation (Figure 4E). These data demonstrate maintenance and expansion of genome edited pHSCs and progenitors from adult donors under low cytokine conditions and provide a potential therapeutic methodology to ensure robust transplantation of $CD34^+$ products in SCD patients undergoing curative gene therapy.

Discussion

Ex vivo expansion of human HSCs from UCB has tremendous therapeutic potential for hematopoietic malignancies and bone marrow failure, but a major challenge has been the loss of self-renewing HSCs when cells are stimulated with hematopoietic cytokines. Similarly, gene therapy for inherited blood disorders such as sickle cell disease has been limited by the low recovery of functional HSCs, which may also be due, in part, to high cytokine exposure. Cytokines increase anabolic processes including protein synthesis, which must be restricted to maintain the capacity for self-renewal in HSCs[42,43]. Thus the increase in translation associated with a high level of cytokine signaling may be detrimental to the expansion of functional, long-term HSCs[1,2,42-48]. Our approach limits cytokine exposure (both concentration and duration) and reduces translation initiation, achieving five-fold expansion of long-term HSCs. These conditions also allow ex vivo expansion of adult human HSCs after CRISPR/Cas9 mediated gene editing of the *BCL11A+58* enhancer, potentially overcoming a major obstacle to gene therapy for sickle cell disease, thalassemias, and other inherited blood disorders.

Other promising approaches for ex vivo HSC expansion are at various stages of development[18-32,34,35]. Our method is distinct from those approaches because we have reduced cytokine exposure substantially. Although the reduced cytokine exposure results in modest (five-fold) HSC expansion, this should be more than sufficient to allow use of the many stored UCB units that are just under the threshold of $CD34^+$ cell counts for clinical use. Indeed, a two-fold expansion should, in principle, be equivalent to the clinically used double cord approach, and would avoid the problem of immunological extinction of cells from one of the two donors.

Single cell analysis of cord blood cells enriched for HSCs revealed several interesting features. As expected, flow sorted $CD34^+CD38^-CD45RA^-CD90^+$ cells at day 0 are heterogeneous, with at least four types of cells in addition to the HSP/MPP population. Importantly, the HSC/MPP population is maintained when cells are cultured with inhibitors of GSK-3 and mTORC1, but not with control medium, consistent with our prior studies showing that functional HSCs are maintained under cytokine-free conditions. HSC/MPPs were also maintained (but not expanded) when low dose cytokines were added. Thus, an HSC/MPP transcriptomic signature is maintained in parallel with long-term self-renewal in our cytokine-free conditions as well as in the presence of low dose cytokines.

Remarkably, the most highly upregulated gene in the HSC/MPP population was the unfolded protein response sensor *GRP78/HSPA5*[50]. Multiple IER genes and several *JUN* family transcription factors, which mediate IER gene activation and stress responses that signal through JUN kinases (JNKs), were also significantly increased in HSC/MPPs. These observations are consistent with prior work showing that UPR components are enriched in HSCs and essential for maintaining HSC self-renewal during hematopoietic stress[1,42,45,58].

Among its many functions, mTORC1 activates translation but the mRNA targets of mTORC1 regulation are surprisingly limited. mRNAs with 5' polypyrimidine tracks are particularly sensitive to inhibition by Rapamycin[59]. Similarly, concentrations of 4E1RCat that enhance HSC expansion only partially inhibit translation. This could indicate that a subset of mRNAs has higher sensitivity to 4E1RCat, but, alternatively, the partial reduction in translation with 4E1RCat may improve HSC maintenance by reducing overall proteostatic stress. Consistent with this interpretation, partial reduction in unfolded proteins in the endoplasmic reticulum improves HSC fitness and, conversely, increased misfolded protein impairs in vivo repopulation in human:mouse xenografts[42,45]. Similarly, small increases in the rate of protein synthesis impair

HSC function[43]. Thus, the HSC expansion we observe with modest reduction in global protein synthesis by 4E1RCat may be due to a reduction in proteostatic stress.

In summary, we have identified a protein synthesis inhibitor that, in combination with low cytokine exposure, confers five-fold expansion of human HSCs from umbilical cord blood. This degree of expansion is modest by intention, and is more than sufficient to make a large number of stored UCB units available for HSCT. This degree of expansion would also surpass the quantity of $CD34^+$ cells used clinically in "double cord" HSCT. This approach may benefit patients from genetic and ethnic backgrounds that are not well represented in bone marrow registries and those who are not suitable for haploidentical transplants. Furthermore, the approach may overcome a major obstacle to gene therapy for inherited blood disorders by maintaining and expanding HSCs after gene editing.

Online Methods

Human umbilical cord blood $CD34^+$ cell culture

Human $CD34^+$ cells from umbilical cord blood pooled from 10 mixed donors per vial were obtained from the STEMCELL Technologies (CAT# 70008) and cultured in StemSpan™ SFEM II (STEMCELL Technologies). CHIR99021 and rapamycin (Cayman Chemical) reconstituted in DMSO were added to final concentrations of 3 μM (CHIR99021) and 5 nM (rapamycin) for all experiments (designated CR medium). Low concentration cytokine medium with CR (CRCY) included 12.5 ng/ml human stem cell factor (SCF), 12.5 ng/ml human Thrombopoietin (TPO), 1.25 ng/ml human IL3. 4E1RCat (Selleckchem), 4E2RCat (MedchemExpress), and 4EGI-1(Selleckchem) were reconstituted in DMSO and used at the concentrations indicated. $CD34^+$ cells were distributed into 96-well U-bottom plates at 50,000 cells per well with 200 μl medium. Except as described for the HTS, one-half volume of medium was replaced every other day. After 7 days (37ºC, 5%CO_2), the total culture product was harvested, and cells were washed and detected by flow cytometry or transplanted into NSG mice.

Single-cell RNA-seq

$CD34^+CD38^-CD45RA^-CD90^+$ cells were purified from $CD34^+$ UCB cells by fluorescence activated cell sorting (FACS) and cultured in StemSpan SFEM with vehicle control (DMSO), CR, or CRCY. After two days, the cultured samples and freshly thawed and sorted $CD34^+CD38^-CD45RA^-CD90^+$ cells (uncultured/day 0) from the same lot number/pool of cells used for culture were collected and single cells were isolated using the 10XGenomics platform; cDNA libraries were prepared according to 10XGenomics user manual using Chromium Single Cell 3' Reagent Kits v3 (10X Genomics) through the the Center for Applied Genomics, Children's Hospital of Philadelphia. Next generation sequencing was performed by Genewiz. Cell Ranger (10X Genomics) was used to process the scRNA-seq data. Cell Ranger Count aligned the sequencing reads to the human reference genome (hg38) using STAR. The output files for the two replicates were aggregated into one gene-cell expression matrix using Cell Ranger aggr with the mapped read depth normalization option. Subsequent analysis was performed using Seurat (4.3.0.1) in R. Using Read10X function, we obtained unique molecular identifiers (UMI) for each cell in Day 0, CR, CRCY, and DMSO-treated conditions. This analysis identified 10364 cells in the Day 0 group, 11771 cells in the CR group, 10519 cells in the CRCY group, and 4884 cells in the DMSO group. Quality control was performed to remove low quality cells. We filtered out cells that contained less than 700 unique feature counts and cells that contained more than 10% mitochondrial counts. After filtering, Day 0 contained 8571 cells, CR contained 8683 cells, CRCY contained 10282 cells, and DMSO contained 3080 cells.

SCTransform function (method = "glmGamPoi") was applied to normalize and scale the gene expression within each condition. The effect of mitochondria was removed using vars.to.regress

= c("percent.mt"). SelectIntegrationFeatures function (nfeatures = 3000) was performed to select features for integration. PrepSCTIntegration function was used to prepare SCTransform gene expression for integration and FindIntegrationAnchors function (reference = UC) and IntegrateData function detected anchors and integrated cells from each condition. RunPCA function was used to generate principal component analysis (PCA) and the RunUMAP function was used to reduce the dimensions of the integrated dataset into 2-D space. The FindNeighbors function was performed to find k-nearest neighbours (KNN) for each cell, and FindCluster function was performed to group cells basis of KNN into cluster using the Louvain algorithm (resolution = 0.1,0.3,0.5,0.8,1,2,3), and resolution = 0.3 was picked in clustering cells. Cells were annotated based on gene markers defined by Zheng et al[60] and HumanPrimaryCellAtlasData library. After running PrepSCTFindMarkers function, we used FindAllMarkers function to identify differentially expressed genes among each cluster. HSC/MPP signature genes were found using FindMarkers function. Finally, we used FindConservedMarkers function to confirm HSC/MPP signature genes among all conditions. scRNA-seq data were deposited in the NCBI Gene Expression Omnibus[61] and are accessible through GEO Series accession number GSE248311.

Gene ontology analysis

Gene ontology analysis was performed using Metascape (https://metascape.org).

High throughput screen

The HTS screen was performed through the High Throughput Screening Core facility at the Perelman School of Medicine. Human UCB $CD34^+$ cells in CRCY (StemSpan SFEM with 3 μM (CHIR99021), 5 nM (rapamycin) and 12.5 ng/ml human stem cell factor (SCF), 12.5 ng/ml human Thrombopoietin (TPO), 1.25 ng/ml human IL3) were distributed into 384-well plates at 1000 cells per well where each well contained one compound. Cells were similarly distributed into at least 16 empty wells/plate as vehicle controls. After 4 days of culture (37ºC, 5%CO_2), cell number was measured indirectly using the Luminescence ATP Detection Assay System kit as directed by the manufacturer (PerkinElmer). Luminescence was detected by an EnVision Xcite multi-plate reader (PerkinElmer).

Fluorescence activated cell sorting (FACS) and flow cytometric analysis

For phenotypic HSC (pHSC) detection, freshly thawed (Day 0) or cultured human $CD34^+$ cells are incubated with Alexa Fluor 700 anti-human CD34 antibody (CAT# 343622, Biolegend), Brilliant Violet 421™ anti-human CD38 antibody (CAT# 356618, Biolegend), APC/Cyanine7 anti-human CD45RA antibody (CAT# 304128, Biolegend), Alexa Fluor 488 anti-human CD49f antibody (CAT# 313608, Biolegend), BUV395 anti-human CD90 (CAT# 563804, BD Biosciences), and LIVE/DEAD™ Fixable Aqua Dead Cell Stain (CAT# L34965, ThermoFisher Scientific). Analyses were performed on LSRFortessa flow cytometers (Becton Dickinson). Data were analyzed using FlowJo 10.9.0. Sorting was performed on the BD Influx™ cell sorter.

Assessment of rate of translation

Human $CD34^+$ cells were cultured as described above for 24 h, and then O-propargylpuromycin (OP-Puro; Click-iT™ Plus OPP Alexa Fluor™ 647 Protein Synthesis Assay Kit, ThermoFisher Scientific) was added (10 μM) to the medium for an additional 60 min. Cells were washed with PBS and stained with surface markers indicated. BD Cytofix/Cytoperm™ Fixation/Permeabilization Kit (CAT# 554714) were used for the fixation and permeabilization of cells. Cells were incubated in 250 μl BD Fix/Perm solution for 20 min covered on ice. Then cells are incubated in 1ml of 1x BD Perm/Wash buffer at room temperature for 15 minutes. The azide-alkyne cycloaddition was performed using the Click-iT™ Plus OPP Alexa Fluor™ 647 Protein Synthesis Assay Kit as directed by the manufacturer. After the 30-min reaction, cells

were washed in PBS supplemented with 2.5 % FBS, then stained for surface markers indicated and analyzed by LSRFortessa flow cytometers (Becton Dickinson). Data were analyzed using FlowJo 10.9.0.

Colony-forming unit (CFU) assay

For CFU assays, 100 day 0 or cultured CD34$^+$ cells were mixed with 1 ml semi-solid methylcellulose medium MethoCult™ H4435 Enriched (STEMCELL Technologies) by shaking vigorously for one minute, incubated for 10 minutes to dissipate bubbles, and plated in 6-well SmartDish™ plates (STEMCELL Technologies) using a blunt-end needle and syringe. Sterilized water or phosphate buffered saline were added to empty wells to provide humidity. After 14 days, colonies were counted by STEMvision™ Hematopoietic Colony Counter (STEMCELL Technologies).

Transplantation into NSG mice

Transplants into NSG mice were performed by the Stem Cell and Xenograft Core Facility at Perelman School of Medicine at the University of Pennsylvania). All animal experiments were performed in accordance with guidelines approved by the Institutional Animal Care and Use Committee (IACUC) at the University of Pennsylvania. Transplant recipients were 8- to10-week-old females. For primary transplants, Day 0 or cultured human CD34$^+$ cells were injected into NSG mice conditioned with busulfan 24 hours prior by intravenous (IV) injection. The cell number injected was based on the number of cells seeded into the wells at day 0 (equal volume of cells injected from day 0 and day 7). Bone marrow was collected by aspiration at 20 weeks and red cells were lysed with Ammonium Chloride Solution (STEMCELL Technologies). Mononuclear cells were stained with PE anti-human CD45 antibody (CAT# 368510, Biolegend), APC/Cyanine7 anti-mouse CD45 antibody (CAT# 103116, Biolegend), APC anti-human CD3 antibody (CAT# 317318, Biolegend), PerCP/Cyanine5.5 anti-human CD19 antibody (CAT# 302230, Biolegend), FITC anti-human CD33 antibody (CAT# 366620, Biolegend), Alexa Fluor 700 anti-human CD34 antibody (CAT# 343622, Biolegend), and PE/Cyanine7 anti-human CD38 antibody (CAT# 397114, Biolegend) and human cell engraftment and multilineage reconstitution were assessed by flow cytometry. The frequency of HSCs was calculated using Extreme Limiting Dilution Analysis (ELDA) software (https://bioinf.wehi.edu.au/software/elda/) from the Bioinformatics Division, the Walter and Eliza Hall Institute of Medical Research).

For serial transplantation, bone marrow was harvested from primary recipients by terminal harvest and extrusion from femurs and tibias at 29 weeks, and 10 × 10^6 bone marrow cells were transplanted into each busulfan conditioned secondary recipient. After 18 weeks, bone marrow was collected and analyzed with PE anti-human CD45 antibody (CAT# 368510, Biolegend), APC/Cyanine7 anti-mouse CD45 antibody (CAT# 103116, Biolegend), APC anti-human CD3 antibody (CAT# 317318, Biolegend), BB515 Mouse anti-Human CD33 (CAT# 564588, BD Biosciences), BB700 mouse anti-Human CD19 (CAT# 566396, BD Biosciences), Brilliant Violet 421™ anti-human CD41 antibody (CAT# 303730, Biolegend), BUV395 Mouse anti-Human CD235a antibody (CAT# 563810, BD Biosciences), PE/Cyanine7 anti-human CD34 antibody (CAT# 343616, Biolegend), and Brilliant Violet 711™ anti-human CD38 antibody (CAT# 303528, Biolegend). Analyses were performed on LSRFortessa flow cytometers.

Culture of mobilized peripheral blood CD34$^+$ cells

Human CD34$^+$ cells from peripheral blood of healthy donors were obtained from the Cooperative Centers of Excellence in Hematology Core at the Fred Hutchinson Cancer Center. Cells were thawed and cultured in CRCY±4E1RCat as described above. For erythroid differentiation, an established 3 phase erythroid culture system was used[62]. For Phase I, cells were cultured for 8 days in Iscove's Modification of DMEM (IMDM) (Mediatech, #MT10016CV)

supplemented with 100 ng/mL human SCF (Peprotech, #300-07), 1 ng/mL IL-3 (Peprotech, #200-03), 3 units/mL erythropoietin (Amgen, #55513-144-10), 200 µg/mL holo-transferrin (Sigma, #T4132), 5% human AB serum (Sigma, #H4522), 2% penicillin/streptomycin (ThermoFisher, #15140122), 10 µg/mL heparin (Sigma, #H3149), and 10 µg/ml insulin (Sigma, #I9278). IL-3 was then withdrawn (Phase 2) and cells were cultured for 5 days. For Phase III, the cells were cultured for 2 days with IMDM supplemented with 3 units/mL erythropoietin, 2% penicillin/streptomycin, 1 mg/mL holo-transferrin, 10 µg/ml insulin, 5% human A/B plasma and 10 µg/mL heparin.

RNP electroporation

CRISPR-Cas9 RNP electroporation was performed as previously described[62,63]. Briefly, RNP complexes were assembled by combining 300 pmol modified sgRNA (Synthego) and 50 pmol HiFi SpCas9 protein (IDT #1081061) and incubated at room temperature for 15 minutes. $CD34^+$ cells (200,000 cells) in CRCY were electroporated 6 hours after thawing in 25 µL total volume using the P3 Primary Cell 4D-NucleofectorTM X Kit (#V4XP-3032) on the Amaxa 4D Nucleofector (Lonza) with program DZ-100. The sgRNA sequence used to target the erythroid-specific BCL11A+58 enhancer was 5'-CTAACAGTTGCTTTTATCAC-3'.

HbF and erythroid differentiation flow cytometry

HbF and erythroid differentiation analyses were performed as previously described[63]; briefly, 1.5 million cells at day 15 of culture were washed in PBS, fixed with 0.05% glutaraldehyde (Sigma #G6257), permeabilized with 0.1% Triton X-100 (Life Technologies #HFH10) and stained with AF647 HbF (Novus Biologicals #NB110-41084) at 1:200 dilution and PE-CD71 (Biolegend, #334106) and PE-Cy7 CD235a (Biolegend, Cat. #306620) at 1:100 dilution. Flow cytometry was carried out on a FACSCanto analyzer (Becton Dickinson) and analyzed with FlowJo 10.9.0 software.

Statistical methods

Statistical analysis was performed using Prism version 10 software. Comparisons of multiple treatment groups were analyzed by one-way ANOVA. Comparisons of two treatment groups were analyzed by 2-tailed Student's t test. Results were considered significant when $P < 0.05$. Statistical analysis of limiting dilution assays was performed using ELDA software.

Conflict of Interest: The authors declare no conflict of interest.

Acknowledgements: We thank Dr. Ana Domingo Muelas for help with graphics and Dr. Ivan Maillard for comments on the manuscript.

Funding: PSK was funded by grants from the National Institutes of Health (R01HL141759), the Penn-CHOP Blood Center, the Institute for Translational Medicine and Applied Therapeutics (ITMAT), and the Institute for Regenerative Medicine (IRM) at the Perelman School of Medicine at the University of Pennsylvania. JH was funded by a grant from the NHLBI (R01HL157118). GAD was funded by NIH grant# 2R01HL119479. JRA-D was supported by grants from the NIH (K01DK129442 and DP1DK130673) and the Human Islet Research Network (U24DK104162). SAP was supported by a grant from the NIH (K08DK129716), the Doris Duke Charitable Foundation Physician Scientist Fellowship (2020062), and an American Society of Hematology Scholar Award. Mobilized adult CD34+ cells were provided by the Cooperative Centers of Excellence in Hematology at Fred Hutchinson Cancer Research Center, which is supported by the NIDDK (DK106829).

Supplemental data

1. Supplemental Figures 1-4
2. Supplemental Table 1: Differential gene expression in specific populations
3. Supplemental Table 2: GO metascape
4. Supplemental Table 3: HTS data summary

Figure Legends

Figure 1. Maintenance of HSC/MPP gene signature in low cytokine culture conditions. A. HSCs were enriched from UCB CD34$^+$ cells by purifying CD34$^+$CD38$^-$CD45RA$^-$CD90$^+$ cells, which contain ~5-10% functional HSCs[49,64,65], and were then cultured in cytokine-free medium with CHIR99021 and Rapamycin (CR), CR with low dose cytokines (CRCY), or control medium (DMSO) for 2 days and subjected to single cell RNA-seq. Freshly sorted cells (day 0) were isolated at the same time. HSC/MPP, CMP, MEP, LMPP and early erythroid commitment populations were identified based on previously published data[60] and visualized by uniform manifold approximation and projection (UMAP). Each dot represents one cell and colors represent cell clusters as indicated. **B.** Number of cells in HSC/MPP, CMP, MEP, LMPP, and early erythroid commitment populations at day 0 or after culture in control (DMSO), CR, or CRCY media. **C.** Scorecard dot plot showing top 5 enriched genes within HSC, CMP, MEP, LMPP and early erythroid commitment populations. Diameter of circle represents percent of cells expressing each marker and color indicates relative expression in the respective populations. **D.** UMAP feature plot showing enrichment of HSPA5/GRP78 in the HSPC population. **E.** Gene Ontology (GO) enrichment analysis of HSCs signature genes compared to other populations. Bar graph shows significantly enriched pathways, with Fisher's exact test -log [q value] on X-axis.

Figure 2. Small molecule inhibitors of translation initiation enhance ex vivo expansion of human pHSCs. A. HTS workflow: Human UCB CD34$^+$ cells were added to 384 well dishes with vehicle (DMSO) or test compound from the Selleck bioactive compound library (>2240 compounds) in CRCY, cultured for 4 days, and cell number measured by ATP bioluminescence. **B.** Waterfall plot representing cell number as a percentage of control (DMSO) for each compound. Screen was performed twice at 1 μM and once at 0.1 μM and compounds identified as > 140% of control (Red box) in all 3 screens were selected for further study. 4E1RCat and 4EGI-1 are highlighted by red dots. **C.** CD34$^+$ cells from UCB were cultured for 7 days in CRCY with vehicle (DMSO) or with increasing concentrations of 4E1RCat (500 nM, 2 μM, 10 μM), 4E2RCat (100 nM, 1 μM, 10 μM), or 4EGI-1 (1 μM, 10 μM) and then CD34$^+$CD38$^-$CD45RA$^-$CD90$^+$CD49f$^+$ (pHSCs) cells were detected by flow cytometry. The number of pHSCs after 7 days of culture is shown relative to the number at day 0 (freshly isolated cells). Data for day 0, DMSO, and 4E1RCat represent the mean values from 6 biological replicates (6 samples of mixed donors). Data for 4E2RCat and 4EGI-1 show mean of 3 replicates (3 distinct mixed donors). * indicates $p < 0.05$, ** indicates $p < 0.01$, *** indicates $p < 0.001$, ****indicates $p < 0.0001$. (one- way ANOVA). **D.** Colony forming units (CFU) were measured in uncultured (Day 0) CD34$^+$ cells and cells cultured for 7 days in CRCY with vehicle (DMSO) or 4E1RCat (2 μM). Total number of mixed cell lineage CFUs or CFU-GEMM (granulocyte, erythrocyte, monocyte, megakaryocyte), CFU-G/M/GM (granulocyte, macrophage, granulocyte/macrophage) and BFU-E (burst forming units-erythroid) are shown in the left panel. **E.** Data from panel D showing multipotent progenitors as CFU-GEMMs with an expanded y-axis. Data show results from 3 distinct mixed donors UCB samples. ****indicates $p < 0.0001$. Statistical significance was calculated by one- way ANOVA. NS, not significant. **F.** Inhibition of translation by 4E1RCat: CD34$^+$CD38$^-$CD90$^+$ cells were cultured in CRCY and increasing concentrations of 4E1RCat (0 μM, 2 μM, 5 μM, 10 μM) and translation was measured by OP-Puro incorporation and flow cytometry. **G.** OP-Puro fluorescence is shown as relative median fluorescence intensity. *** indicates $p < 0.001$, ****indicates $p < 0.0001$. (one- way ANOVA).

Figure 3. 4E1RCat promotes expansion of LT-HSCs. A. Limiting dilution analysis (LDA) of human UCB CD34$^+$ cells at day 0 or after 7 days of culture in CRCY+DMSO or CRCY with 4E1RCat (2 μM). Dose of cells injected is based on the number of CD34$^+$ cells on day 0.

Chimerism was measured as human $CD45^+$ cells at 20 weeks in bone marrow with engraftment defined as ≥ 0.1% $hCD45^+$. Data are from 2 distinct LDA/transplant experiments. **B.** HSC frequency with 95% CI calculated with ELDA software. p = 0.001 for CRCY+4E1RCat compared to fresh cells. No significant difference for CRCY+DMSO compared to Day 0 cells. **C-F.** The percentage of human T cells ($CD3^+$ cells), B cells ($CD19^+$ cells), myeloid cells ($CD33^+$ cells), and lineage negative ($CD34^+CD38^-$) cells is shown for recipients injected with cells from ex vivo cultures corresponding to 5000, 500, 100, 25 $CD34^+$ cells on day 0. **G.** Scheme for secondary transplantation from primary recipients that had received day 0 cells or cells cultured in CRCY+4E1RCat for 7 days. **H.** The percentage engraftment of human $CD45^+$ cells in peripheral blood (16 weeks) in secondary recipients. **I.** The percentage engraftment of human $CD45^+$ cells in the bone marrow (18 weeks) in secondary recipients. **J-N.** The percentage (log_{10} scale) of human lineage negative cells ($CD34^+CD38^-$), B cells ($CD19^+$), myeloid cells ($CD33^+$), megakaryocytes ($CD41^+$) and erythroid cells ($GlyA^+$) in the bone marrow (18 weeks) of secondary recipients. Samples with 0% engraftment are shown at the baseline (with broken y-axes),

Figure 4. Ex vivo expansion of CRISPR modified $CD34^+$ cells. A. Mobilized adult $CD34^+$ cells were edited by CRISPR/Cas9 targeting of the *BCL11A+58* enhancer and then edited cells and non-edited control cells were cultured in CRCY with vehicle (DMSO) or 4E1RCat (100 nM). The absolute number of pHSCs ($CD34^+CD38^-CD45RA^-CD90^+CD49f^+$) in Day 0 (uncultured) and cultured cells is shown. The data represent the mean of replicates from 3 adult donors. * indicates p < 0.05, *** indicates p < 0.001, ****indicates p < 0.0001. NS, not significant. (one-way ANOVA)**. B.** Colony formation was assessed as in Figure 2 for uncultured (Day 0) $CD34^+$ cells and cells cultured for 7 days in CRCY with vehicle (DMSO) or 4E1RCat (100 nM). The data represent replicates from 3 adult donors. **C.** Data from panel B with expanded y-axis to show the number of multipotent progenitors as CFU-GEMMs. **D.** $CD34^+$ cells from Day 0 or after culture in CRCY ± 4E1RCat (100 nM) were cultured to induce erythroid differentiation and HbF expression was assessed by flow cytometry. Flow cytometry histograms are shown for non-edited and edited cells from one adult donor and are representive of results from 3 distinct adult donors. **E.** Erythroid differentiation in freshly isolated (Day 0) cells and cells cultured in CRCY with or without 4E1RCat. Flow cytometry for CD71 (transferrin receptor) and CD235a (glycophorin A) from one adult donor is shown and is representive of results from 3 distinct adult donors.

Supplemental Figure Legends

Supplemental Figure 1. Optimization of screening conditions. A. Human UCB $CD34^+$ cells were added to 384 well dishes in StemSpan SFEM with (red) or without (blue) CR and varying combinations of cytokines as indicated. S: SCF (1 ng/ml), T; Thrombopoietin (100 ng/ml), F: Flt3 ligand (100 ng/ml), I: IL3 (0.1 ng/ml). Cells were cultured for 4 days and cell number measured using a bioluminescence assay (ATPlite). Relative light units (RLU) are shown. Red arrow indicates the combination (STI) selected for the screen. **B.** Varying numbers of $CD34^+$ cells/well and varying concentrations of STI were added to a 384-well dish; cells were cultured for 4 days and cell number measured by bioluminescent assay. Red arrow indicates optimal cell number (1000 cells) and concentration of STI (12.5 ng/ml SCF, 12.5 ng/ml TPO, and 1.25 ng/ml IL3; subsequently referred to as CRCY) selected for HTS. **C.** Validation of screening conditions with CR vs CRCY at two concentrations. **D.** Screen was performed with 1000 cells/well in CRCY in 384 well dishes with 32 control wells (CRCY+DMSO) per plate (lanes 2 and 23) and Selleck library compounds (test) in lanes 3-22. Cells were cultured for 4 days without medium change and cell number was assessed by ATP bioluminescent assay.

Supplemental Figure 2. Multilineage Contribution of HSCs expanded in CRCY+4E1RCat in primary LDA at 20 weeks. The percentage of human $CD45^+$ cells, T cells ($CD3^+$), B cells ($CD19^+$), myeloid cells ($CD33^+$), and $CD34^+CD38^-$ cells in each primary recipient mouse at 20 weeks in bone marrow are represented by a heatmap. Red indicates percentage engraftment (human cells) is > 0.1%. Blue indicates human cell engraftment < 0.1%. White indicates percentage engraftment = 0.1%. Data show results from expansion/transplants using 2 distinct mixed donor UCB samples.

Supplemental Figure 3. Multilineage Contribution of HSCs expanded in CRCY+4E1RCat in primary recipients at 29 weeks. A-E. The percentage of human $CD45^+$ cells, $CD34^+CD38^-$ cells, myeloid cells ($CD33^+$), T cells ($CD3^+$), and B cells ($CD19^+$) at day 29 post-transplant in bone marrow of mice used as donors for secondary transplant. Mice had received either uncultured (Day 0) $CD34^+$ cells or cells cultured in CRCY+4E1RCat for 7 days. **F.** Table showing percent engraftment of each population in each mouse at 29 weeks.

Supplemental Figure 4. Serial transplant of LT-HSCs expanded with CRCY+4E1RCat. Bone marrow harvested from primary recipients at 29 weeks was transplanted into conditioned secondary recipients as described in Figure 3. The percentage of human $CD45^+$ cells was measured in peripheral blood (PB) at 16 weeks. Bone marrow (BM) was harvested at 18 weeks and the percentage of human $CD45^+$ cells T cells ($CD3^+$), B cells ($CD19^+$), myeloid cells ($CD33^+$), megakaryocytic cells ($CD41^+$), erythroid cells ($GlyA^+$) and $CD34^+CD38^-$ cells was measured.

References

1. van Galen, P.*, et al.* Integrated Stress Response Activity Marks Stem Cells in Normal Hematopoiesis and Leukemia. *Cell reports* **25**, 1109-1117 e1105 (2018).
2. Signer, R.A., Magee, J.A., Salic, A. & Morrison, S.J. Haematopoietic stem cells require a highly regulated protein synthesis rate. *Nature* **509**, 49-54 (2014).
3. Purton, L.E. & Scadden, D.T. Limiting factors in murine hematopoietic stem cell assays. *Cell stem cell* **1**, 263-270 (2007).
4. Chou, S., Chu, P., Hwang, W. & Lodish, H. Expansion of human cord blood hematopoietic stem cells for transplantation. *Cell stem cell* **7**, 427-428 (2010).
5. Gragert, L.*, et al.* HLA match likelihoods for hematopoietic stem-cell grafts in the U.S. registry. *The New England journal of medicine* **371**, 339-348 (2014).
6. Lund, T.C., Boitano, A.E., Delaney, C.S., Shpall, E.J. & Wagner, J.E. Advances in umbilical cord blood manipulation-from niche to bedside. *Nat Rev Clin Oncol* **12**, 163-174 (2015).
7. Li, D., Li, X., Liao, L. & Li, N. Unrelated cord blood transplantation versus haploidentical transplantation in adult and pediatric patients with hematological malignancies-A meta-analysis and systematic review. *Am J Blood Res* **10**, 1-10 (2020).
8. Arcuri, L.J., Aguiar, M.T.M., Ribeiro, A.A.F. & Pacheco, A.G.F. Haploidentical Transplantation with Post-Transplant Cyclophosphamide versus Unrelated Donor Hematopoietic Stem Cell Transplantation: A Systematic Review and Meta-Analysis. *Biol Blood Marrow Transplant* **25**, 2422-2430 (2019).
9. Shi, P.A., Luchsinger, L.L., Greally, J.M. & Delaney, C.S. Umbilical cord blood: an undervalued and underutilized resource in allogeneic hematopoietic stem cell transplant and novel cell therapy applications. *Current opinion in hematology* **29**, 317-326 (2022).
10. Gluckman, E.*, et al.* Hematopoietic reconstitution in a patient with Fanconi's anemia by means of umbilical-cord blood from an HLA-identical sibling. *The New England journal of medicine* **321**, 1174-1178 (1989).
11. Laughlin, M.J.*, et al.* Outcomes after transplantation of cord blood or bone marrow from unrelated donors in adults with leukemia. *The New England journal of medicine* **351**, 2265-2275 (2004).
12. Kindwall-Keller, T.L. & Ballen, K.K. Umbilical cord blood: The promise and the uncertainty. *Stem Cells Transl Med* **9**, 1153-1162 (2020).
13. Ballen, K.K., Gluckman, E. & Broxmeyer, H.E. Umbilical cord blood transplantation: the first 25 years and beyond. *Blood* **122**, 491-498 (2013).
14. Li, H.W. & Sykes, M. Emerging concepts in haematopoietic cell transplantation. *Nat Rev Immunol* **12**, 403-416 (2012).
15. Shahrokhi, S., Menaa, F., Alimoghaddam, K., McGuckin, C. & Ebtekar, M. Insights and hopes in umbilical cord blood stem cell transplantations. *J Biomed Biotechnol* **2012**, 572821 (2012).
16. Broxmeyer, H.E. Enhancing engraftment of cord blood cells via insight into the biology of stem/progenitor cell function. *Ann N Y Acad Sci* **1266**, 151-160 (2012).
17. Wagner, J.E., Jr.*, et al.* One-unit versus two-unit cord-blood transplantation for hematologic cancers. *The New England journal of medicine* **371**, 1685-1694 (2014).
18. Chaurasia, P., Gajzer, D.C., Schaniel, C., D'Souza, S. & Hoffman, R. Epigenetic reprogramming induces the expansion of cord blood stem cells. *The Journal of clinical investigation* **124**, 2378-2395 (2014).
19. Fares, I.*, et al.* Cord blood expansion. Pyrimidoindole derivatives are agonists of human hematopoietic stem cell self-renewal. *Science* **345**, 1509-1512 (2014).
20. Boitano, A., E.*, et al.* Aryl hydrocarbon receptor antagonists promote the expansion of human hematopoietic stem cells. *Science* **329**, 1345-1348 (2010).

21. Delaney, C.*, et al.* Notch-mediated expansion of human cord blood progenitor cells capable of rapid myeloid reconstitution. *Nature medicine* **16**, 232-236. (2010).
22. Goessling, W.*, et al.* Genetic interaction of PGE2 and Wnt signaling regulates developmental specification of stem cells and regeneration. *Cell* **136**, 1136-1147 (2009).
23. Guo, B., Huang, X., Lee, M.R., Lee, S.A. & Broxmeyer, H.E. Antagonism of PPAR-gamma signaling expands human hematopoietic stem and progenitor cells by enhancing glycolysis. *Nature medicine* **24**, 360-367 (2018).
24. Hua, P.*, et al.* The BET inhibitor CPI203 promotes ex vivo expansion of cord blood long-term repopulating HSCs and megakaryocytes. *Blood* **136**, 2410-2415 (2020).
25. Rentas, S.*, et al.* Musashi-2 attenuates AHR signalling to expand human haematopoietic stem cells. *Nature* **532**, 508-511 (2016).
26. Kharas, M.G.*, et al.* Musashi-2 regulates normal hematopoiesis and promotes aggressive myeloid leukemia. *Nature medicine* **16**, 903-908 (2010).
27. Clapes, T. & Robin, C. Embryonic development of hematopoietic stem cells: implications for clinical use. *Regen Med* **7**, 349-368 (2012).
28. Wilkinson, A.C.*, et al.* Long-term ex vivo haematopoietic-stem-cell expansion allows nonconditioned transplantation. *Nature* **571**, 117-121 (2019).
29. Perry, J.M.*, et al.* Cooperation between both Wnt/beta-catenin and PTEN/PI3K/Akt signaling promotes primitive hematopoietic stem cell self-renewal and expansion. *Genes & development* **25**, 1928-1942 (2011).
30. Himburg, H.A.*, et al.* Pleiotrophin regulates the expansion and regeneration of hematopoietic stem cells. *Nature medicine* **16**, 475-482 (2010).
31. Zhang, C.C.*, et al.* Angiopoietin-like proteins stimulate ex vivo expansion of hematopoietic stem cells. *Nature medicine* **12**, 240-245 (2006).
32. Horwitz, M.E.*, et al.* Omidubicel vs standard myeloablative umbilical cord blood transplantation: results of a phase 3 randomized study. *Blood* **138**, 1429-1440 (2021).
33. Bai, T.*, et al.* Expansion of primitive human hematopoietic stem cells by culture in a zwitterionic hydrogel. *Nature medicine* **25**, 1566-1575 (2019).
34. Cohen, S.*, et al.* Hematopoietic stem cell transplantation using single UM171-expanded cord blood: a single-arm, phase 1-2 safety and feasibility study. *Lancet Haematol* **7**, e134-e145 (2020).
35. Wagner, J.E., Jr.*, et al.* Phase I/II Trial of StemRegenin-1 Expanded Umbilical Cord Blood Hematopoietic Stem Cells Supports Testing as a Stand-Alone Graft. *Cell stem cell* **18**, 144-155 (2016).
36. Heike, T. & Nakahata, T. Ex vivo expansion of hematopoietic stem cells by cytokines. *Biochimica et biophysica acta* **1592**, 313-321 (2002).
37. Dahlberg, A., Delaney, C. & Bernstein, I.D. Ex vivo expansion of human hematopoietic stem and progenitor cells. *Blood* **117**, 6083-6090 (2011).
38. Sakurai, M.*, et al.* Chemically defined cytokine-free expansion of human haematopoietic stem cells. *Nature* **615**, 127-133 (2023).
39. Nguyen-McCarty, M. & Klein, P.S. Autophagy is a signature of a signaling network that maintains hematopoietic stem cells. *PloS one* **12**, e0177054 (2017).
40. Huang, J., Nguyen-McCarty, M., Hexner, E.O., Danet-Desnoyers, G. & Klein, P.S. Maintenance of hematopoietic stem cells through regulation of Wnt and mTOR pathways. *Nature medicine* **18**, 1778-1785 (2012).
41. Masuda, S., Li, M. & Izpisua Belmonte, J.C. Niche-less maintenance of HSCs by 2i. *Cell research* **23**, 458-459 (2013).
42. van Galen, P.*, et al.* The unfolded protein response governs integrity of the haematopoietic stem-cell pool during stress. *Nature* **510**, 268-272 (2014).
43. Signer, R.A.*, et al.* The rate of protein synthesis in hematopoietic stem cells is limited partly by 4E-BPs. *Genes & development* **30**, 1698-1703 (2016).

44. Kruta, M.*, et al.* Hsf1 promotes hematopoietic stem cell fitness and proteostasis in response to ex vivo culture stress and aging. *Cell stem cell* **28**, 1950-1965 e1956 (2021).
45. Hidalgo San Jose, L.*, et al.* Modest Declines in Proteome Quality Impair Hematopoietic Stem Cell Self-Renewal. *Cell reports* **30**, 69-80 e66 (2020).
46. Burgess, R.J., Zhao, Z., Nakada, D. & Morrison, S.J. Bmi1 suppresses protein synthesis and promotes proteostasis in hematopoietic stem cells. *Genes & development* **36**, 887-900 (2022).
47. Spevak, C.C.*, et al.* Hematopoietic Stem and Progenitor Cells Exhibit Stage-Specific Translational Programs via mTOR- and CDK1-Dependent Mechanisms. *Cell stem cell* **26**, 755-765 e757 (2020).
48. Keyvani Chahi, A.*, et al.* PLAG1 dampens protein synthesis to promote human hematopoietic stem cell self-renewal. *Blood* **140**, 992-1008 (2022).
49. Baum, C.M., Weissman, I.L., Tsukamoto, A.S., Buckle, A.M. & Peault, B. Isolation of a candidate human hematopoietic stem-cell population. *Proceedings of the National Academy of Sciences of the United States of America* **89**, 2804-2808 (1992).
50. Hetz, C. & Papa, F.R. The Unfolded Protein Response and Cell Fate Control. *Molecular cell* **69**, 169-181 (2018).
51. Cencic, R.*, et al.* Reversing chemoresistance by small molecule inhibition of the translation initiation complex eIF4F. *Proceedings of the National Academy of Sciences of the United States of America* **108**, 1046-1051 (2011).
52. Liu, J., Xu, Y., Stoleru, D. & Salic, A. Imaging protein synthesis in cells and tissues with an alkyne analog of puromycin. *Proceedings of the National Academy of Sciences of the United States of America* **109**, 413-418 (2012).
53. Shultz, L.D.*, et al.* Human lymphoid and myeloid cell development in NOD/LtSz-scid IL2R gamma null mice engrafted with mobilized human hemopoietic stem cells. *J Immunol* **174**, 6477-6489 (2005).
54. Bauer, D.E.*, et al.* An erythroid enhancer of BCL11A subject to genetic variation determines fetal hemoglobin level. *Science* **342**, 253-257 (2013).
55. Sankaran, V.G.*, et al.* Human fetal hemoglobin expression is regulated by the developmental stage-specific repressor BCL11A. *Science* **322**, 1839-1842 (2008).
56. Esrick, E.B.*, et al.* Post-Transcriptional Genetic Silencing of BCL11A to Treat Sickle Cell Disease. *The New England journal of medicine* **384**, 205-215 (2021).
57. Frangoul, H.*, et al.* CRISPR-Cas9 Gene Editing for Sickle Cell Disease and beta-Thalassemia. *The New England journal of medicine* **384**, 252-260 (2021).
58. Wey, S., Luo, B. & Lee, A.S. Acute inducible ablation of GRP78 reveals its role in hematopoietic stem cell survival, lymphogenesis and regulation of stress signaling. *PloS one* **7**, e39047 (2012).
59. Jefferies, H.B., Reinhard, C., Kozma, S.C. & Thomas, G. Rapamycin selectively represses translation of the "polypyrimidine tract" mRNA family. *Proceedings of the National Academy of Sciences of the United States of America* **91**, 4441-4445 (1994).
60. Zheng, S., Papalexi, E., Butler, A., Stephenson, W. & Satija, R. Molecular transitions in early progenitors during human cord blood hematopoiesis. *Mol Syst Biol* **14**, e8041 (2018).
61. Edgar, R., Domrachev, M. & Lash, A.E. Gene Expression Omnibus: NCBI gene expression and hybridization array data repository. *Nucleic acids research* **30**, 207-210 (2002).
62. Huang, P.*, et al.* The HRI-regulated transcription factor ATF4 activates BCL11A transcription to silence fetal hemoglobin expression. *Blood* **135**, 2121-2132 (2020).
63. Peslak, S.A.*, et al.* HRI depletion cooperates with pharmacologic inducers to elevate fetal hemoglobin and reduce sickle cell formation. *Blood Adv* **4**, 4560-4572 (2020).

64. Majeti, R., Park, C.Y. & Weissman, I.L. Identification of a hierarchy of multipotent hematopoietic progenitors in human cord blood. *Cell stem cell* **1**, 635-645 (2007).
65. Notta, F*., et al.* Isolation of single human hematopoietic stem cells capable of long-term multilineage engraftment. *Science* **333**, 218-221 (2011).

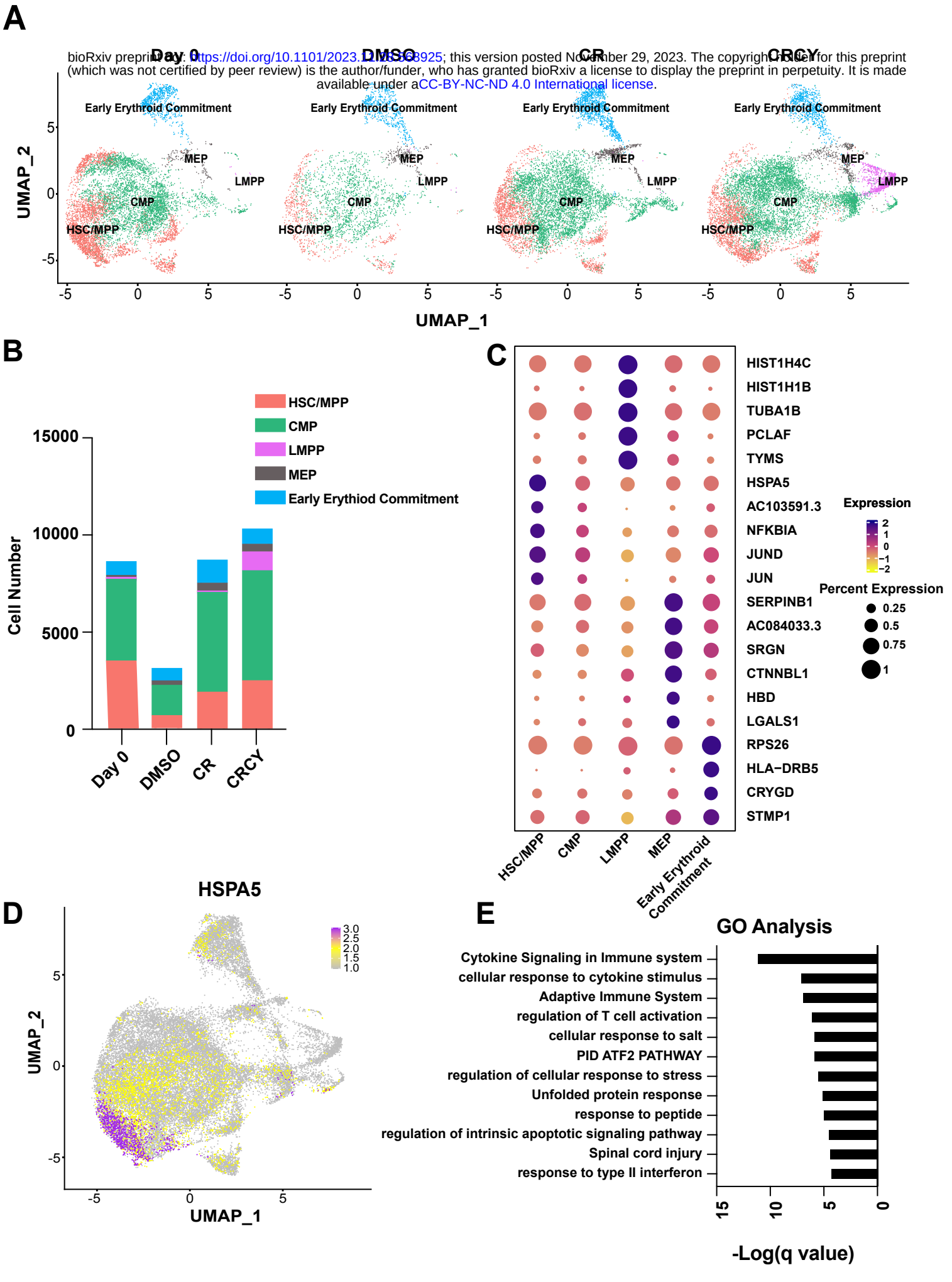

Figure 1

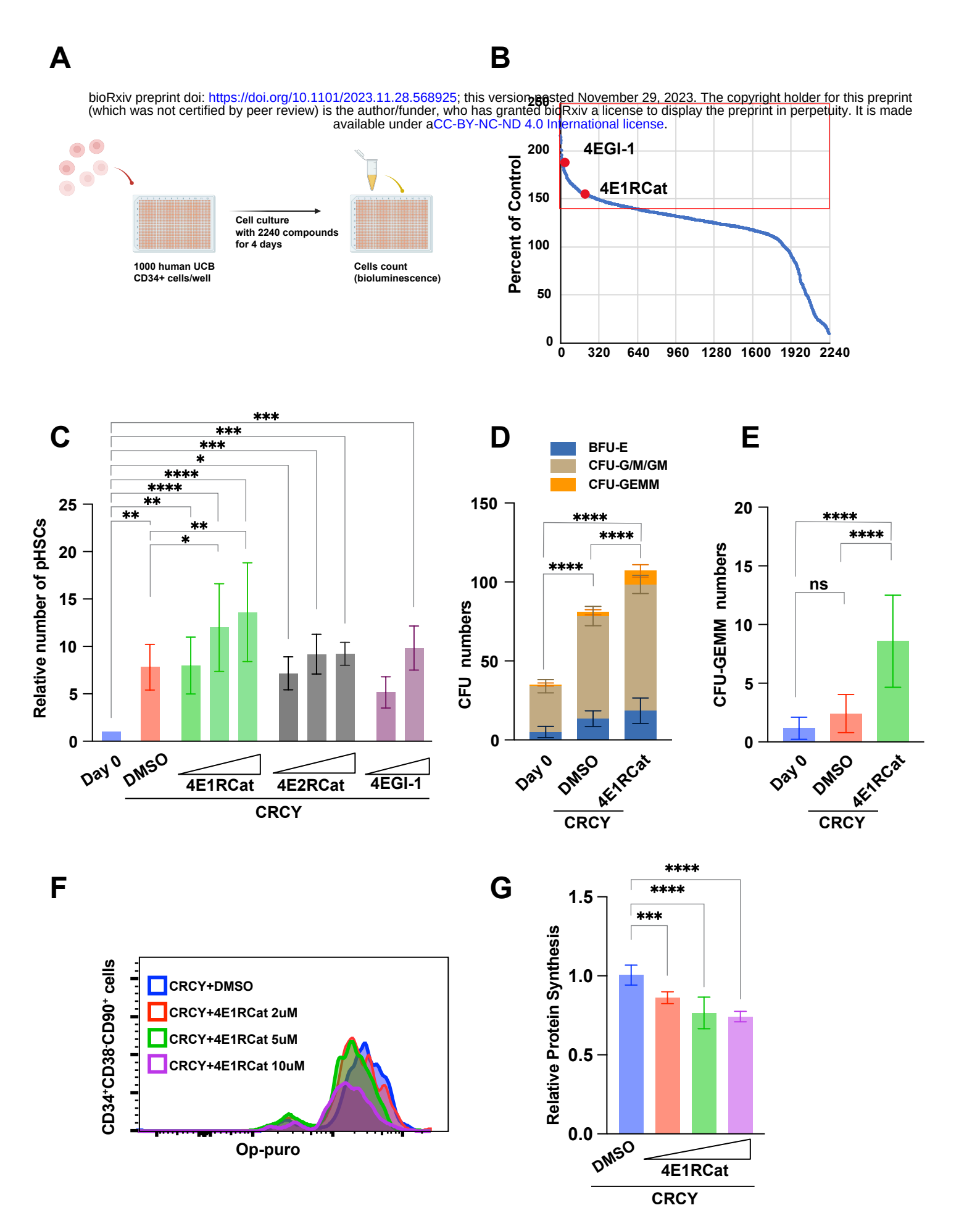

Figure 2

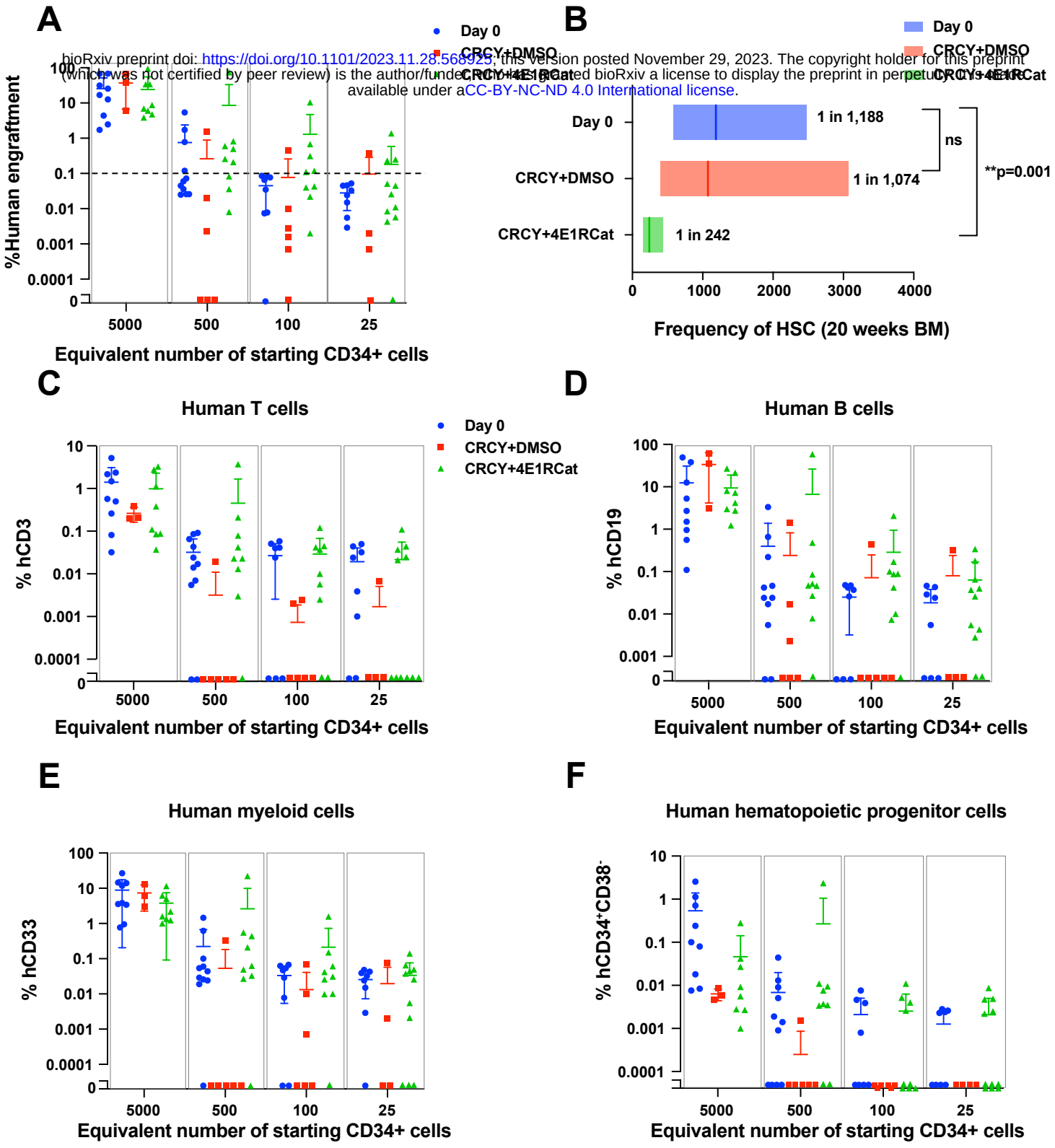

Figure 3

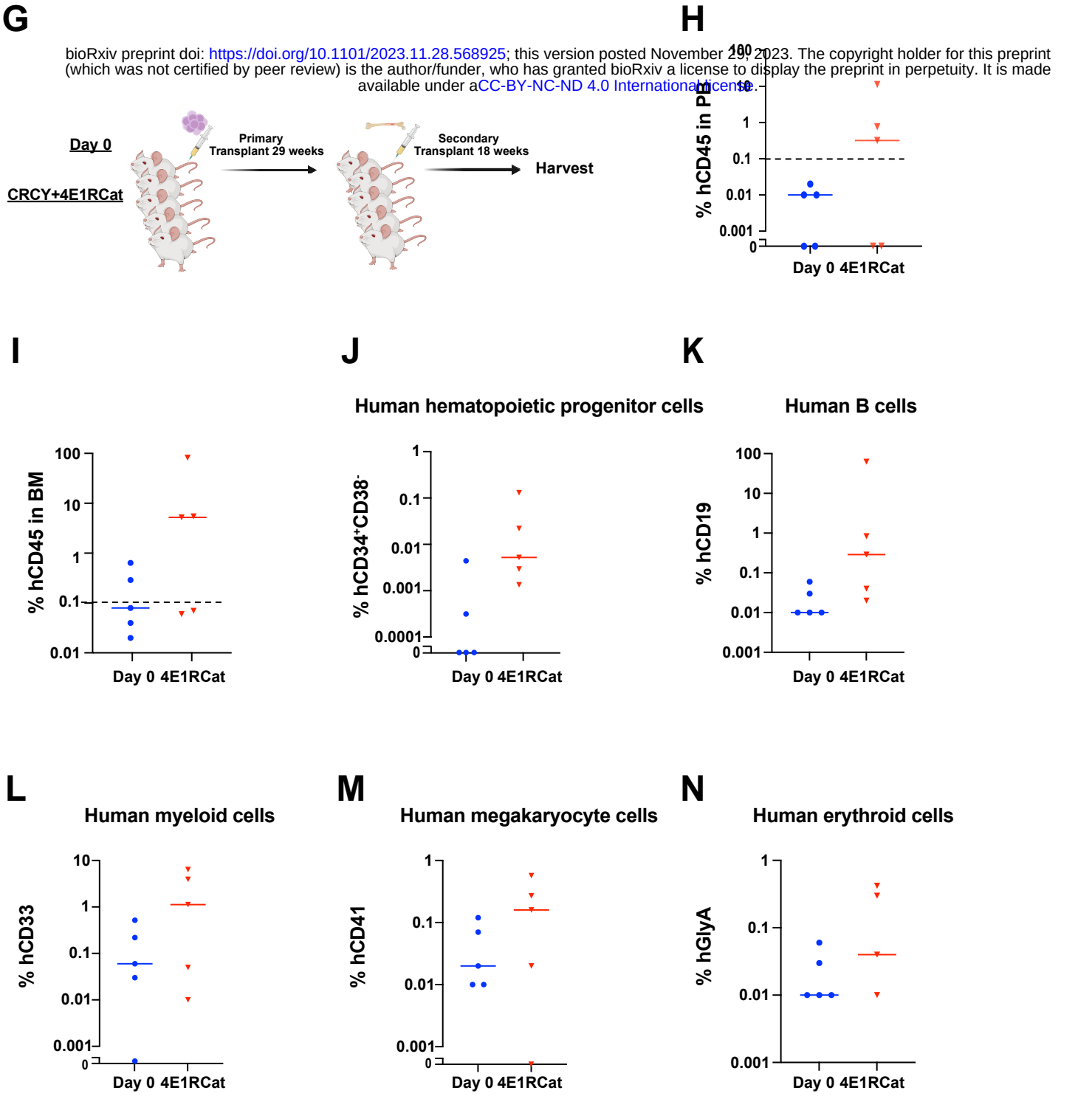

Figure 3

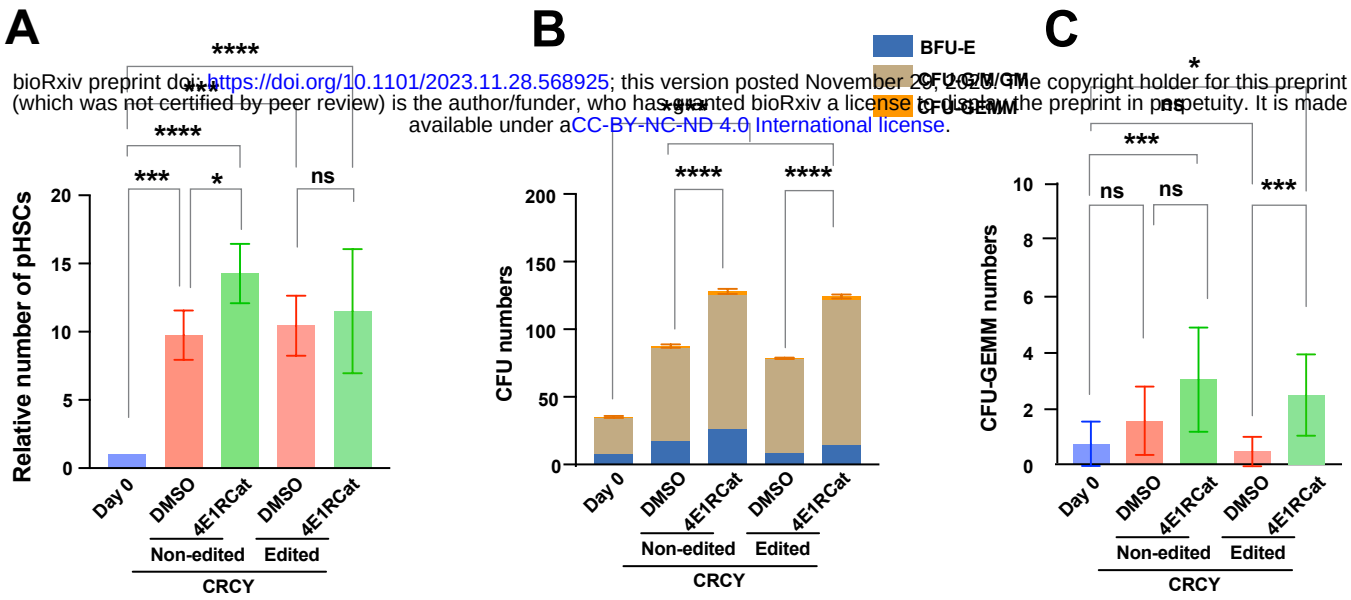

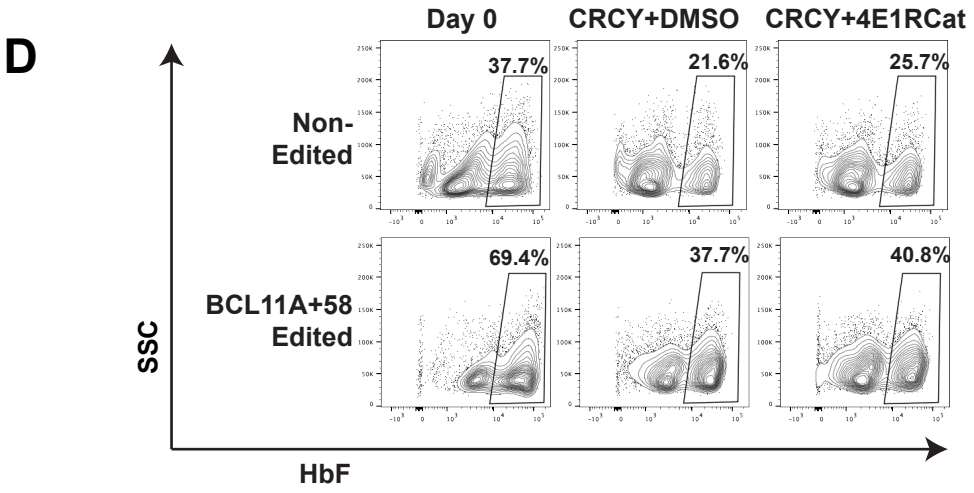

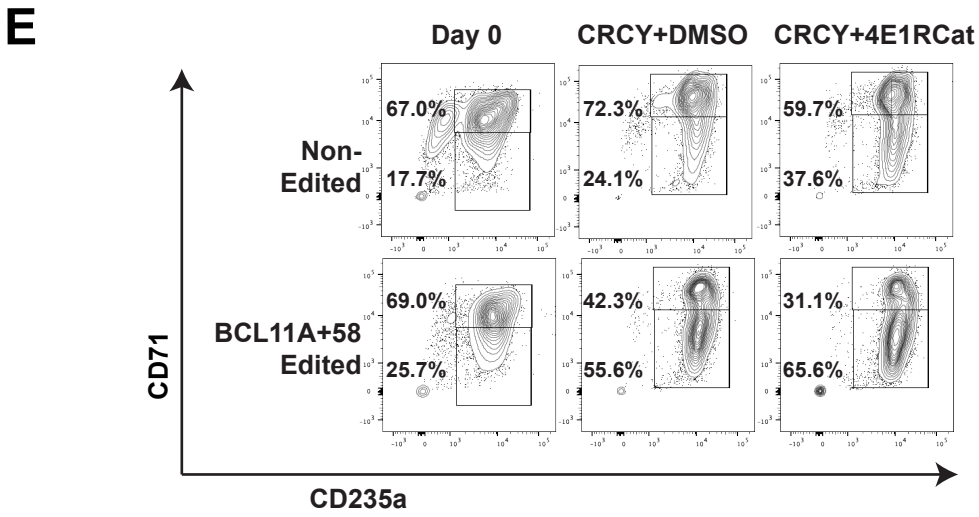

Figure 4

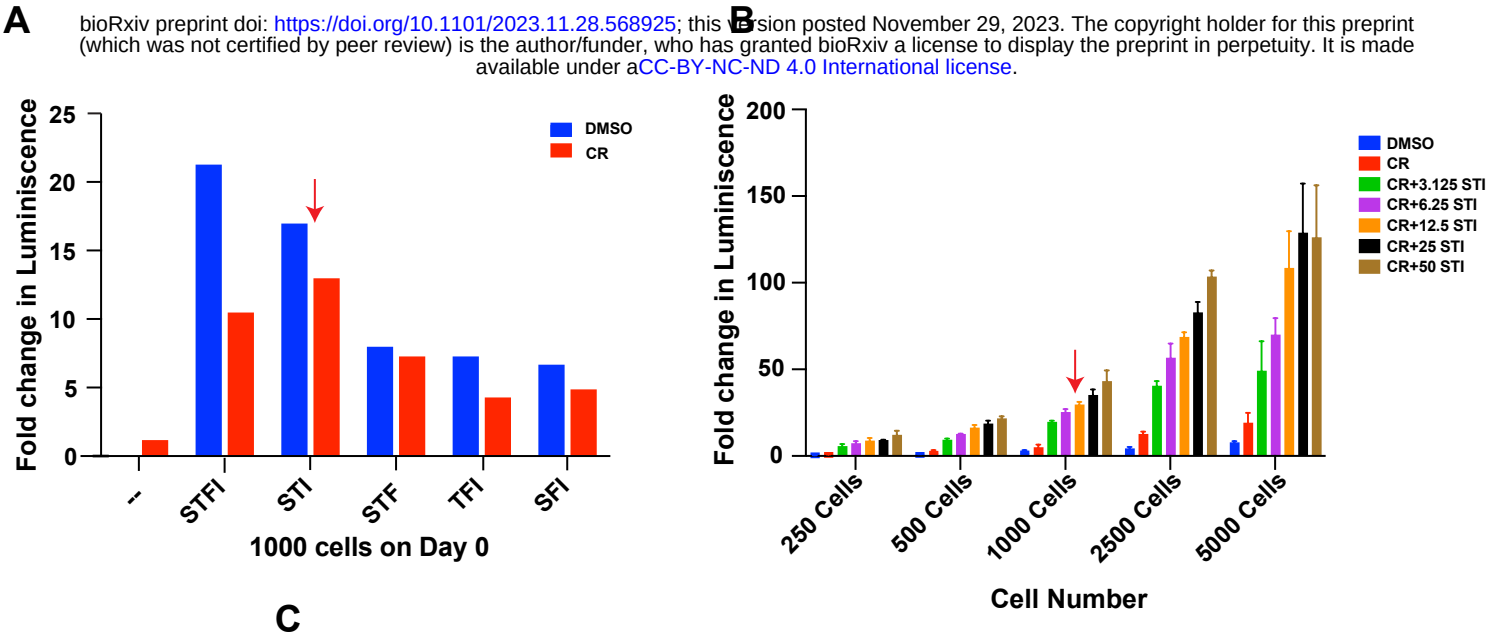

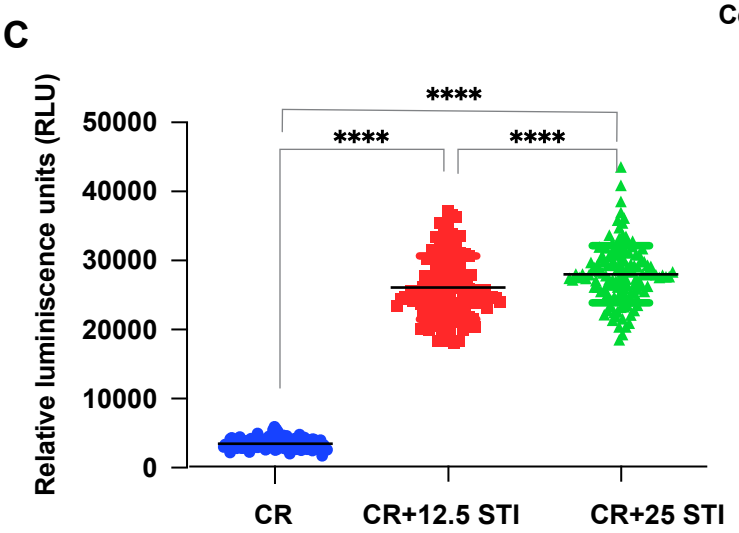

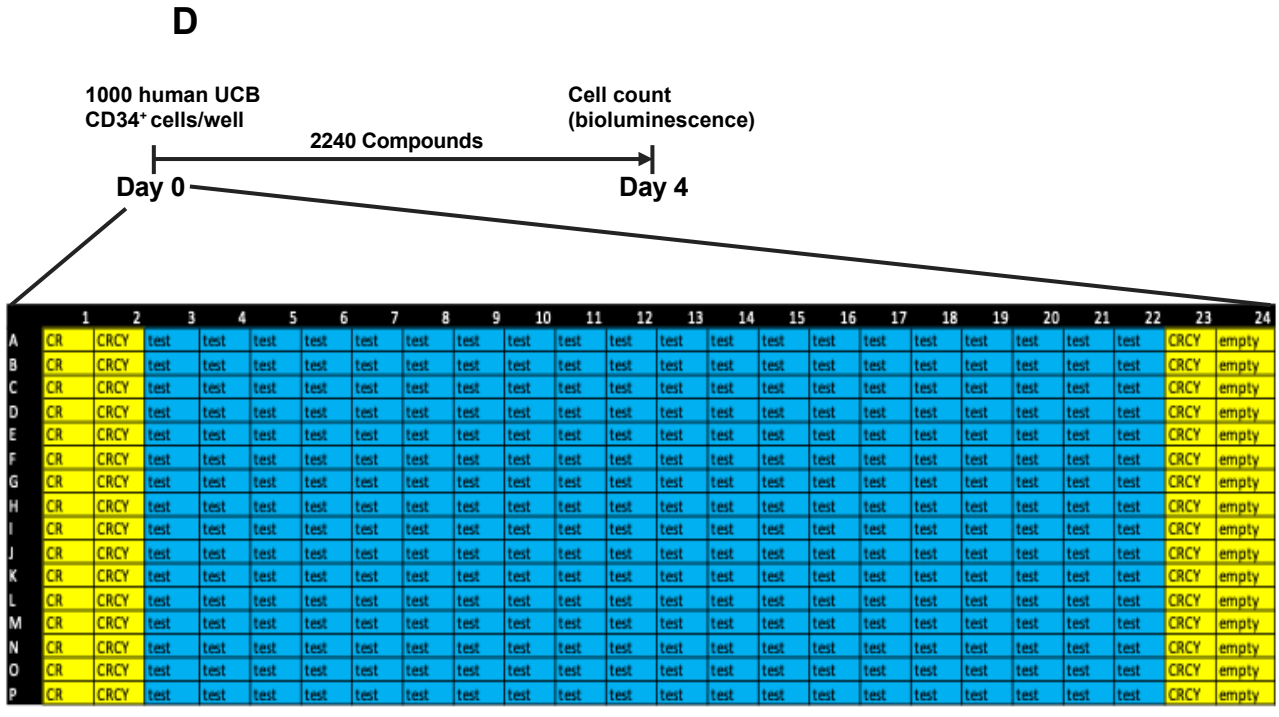

Supplemental Figure 1

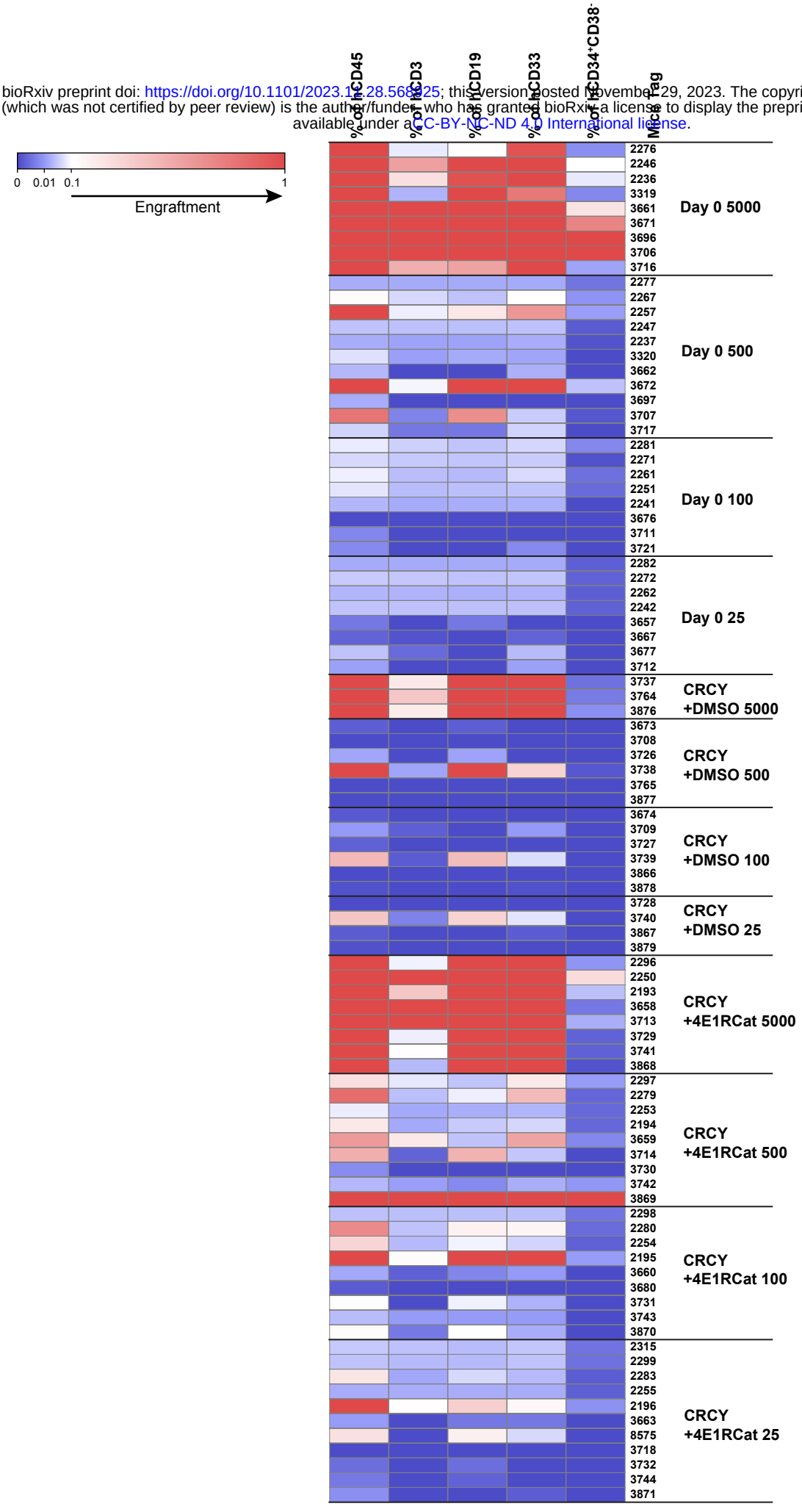

Supplemental Figure 2

A

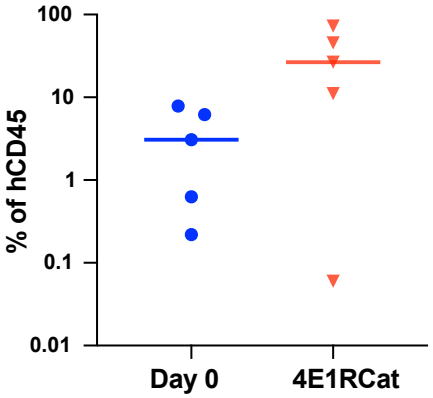

B

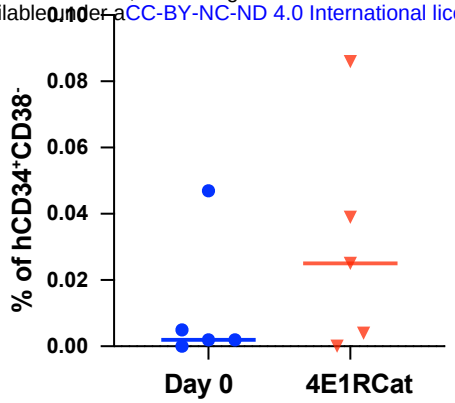

C

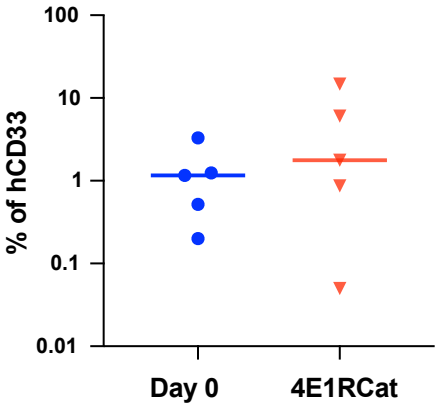

D

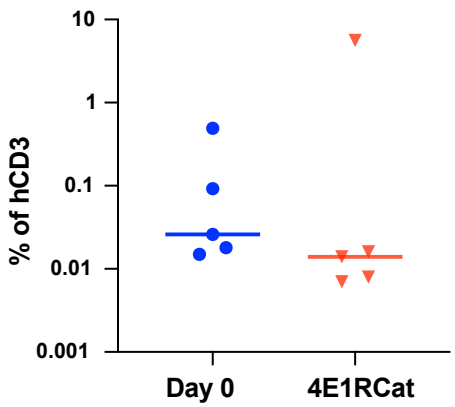

E

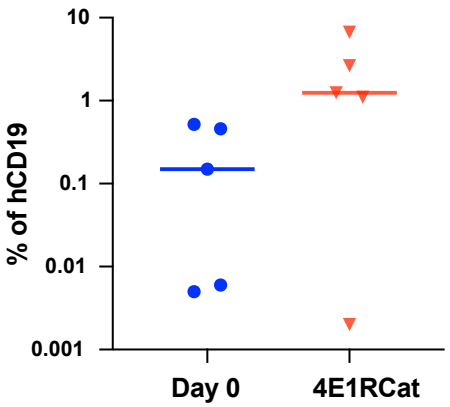

F

Group	Donor Tag #	% of hCD45	% of hCD19	% of hCD33	% of hCD3	% of hCD34+CD38-
Day 0	2276	7.87	0.52	3.3	0.026	0.047
	2246	6.19	0.46	1.24	0.49	0.00455
	2236	3.08	0.15	1.16	0.018	0.00161
	2257	0.63	0.00501	0.52	0.015	0.00167
	2267	0.22	0.00585	0.2	0.092	0
4E1RCat	2296	11.1	1.1	0.87	0.014	0.00434
	2250	45.6	1.24	14.7	5.59	0.039
	2193	72.5	6.68	6.07	0.00744	0.086
	2195	26.6	2.64	1.77	0.0077	0.025
	2196	0.06	0.00162	0.05	0.016	0

Supplemental Figure 3

Group	Donor Tag #	Recipient Tag#	% of hCD45 (PB)	% of hCD45 (BM)	% of hCD3 (BM)	% of hCD19 (BM)
Day 0	2276	2410	0	0.64	0.035	0.056
	2246	2409	0	0.29	0.00442	0.028
	2236	2407	0.00645	0.075	0.00243	0.00729
	2257	2404	0.016	0.04	0.00171	0.00854
	2267	2403	0.00854	0.016	0.00913	0.00913
4E1RCat	2296	2419	0	0.074	0.00586	0.021
	2250	2418	0.32	5.24	1.71	0.29
	2193	2413	11.3	82	0.23	62.7
	2195	2414	0.77	5.49	0.099	0.84
	2196	2416	0	0.064	0.013	0.04

Group	Donor Tag #	Recipient Tag#	% of hCD33 (BM)	% of hCD41 (BM)	% of hGlyA (BM)	% of $hCD34^{+}CD38^{-}$ (BM)
Day 0	2276	2410	0.52	0.12	0.06	0.0044
	2246	2409	0.22	0.069	0.027	0.000316
	2236	2407	0.062	0.021	0.011	0
	2257	2404	0.031	0.011	0.00854	0
	2267	2403	0.00269	0.00591	0.00591	0
4E1RCat	2296	2419	0.051	0.018	0.0088	0.00293
	2250	2418	1.13	0.16	0.3	0.022
	2193	2413	6.38	0.57	0.42	0.13
	2195	2414	3.94	0.27	0.042	0.00521
	2196	2416	0.00935	0.00267	0.00401	0.00134

Supplemental Figure 4